Etude de la convection naturelle dans un thermosiphon constitué de deux parois inclinées à chauffage asymétrique

3.1 Résumé de l'article proposé à Energy & Buildings

Autre que l'isolation des murs d'un bâtiment, les PMR sont également utilisés comme complément d'isolation ou parfois seuls pour isoler les combles. En effet, la plus grande part des déperditions thermiques dans une maison se situant au niveau de la toiture, beaucoup de travaux se sont concentrés sur le développement de solutions techniques au niveau du complexe de toiture afin de diminuer les consommations énergétiques des bâtiments et d'assurer une bonne isolation d'hiver et un confort d'été. Ce chapitre s'intéresse particulièrement à l'étude de la lame d'air ventilée conçue entre la couverture (les tuiles) et l'isolation de la toiture et son impact sur les performances thermiques du complexe de toiture intégrant un produit réfléchissant en été sous l'effet de l'ensoleillement.

En effet, la mise en œuvre de la lame d'air ventilée est conseillée par les DTU de la série 40. Une des fonctions importantes de la lame d'air est l'évacuation de l'humidité qui arrive à passer dans la charpente. Elle a aussi une fonction supplémentaire, celle de limiter l'échauffement des tuiles par la chaleur provenant du rayonnement solaire pour les protéger mécaniquement et augmenter également le confort d'été.

En conditions estivales, l'écoulement dans la lame d'air se fait par effet thermosiphon c'est-à-dire par circulation de l'air de façon naturelle grâce à la variation de la densité du fluide soumis à un gradient de température. Ce mouvement de convection naturelle est fonction de plusieurs paramètres qui sont définis d'après la littérature par le flux solaire incident, l'angle d'inclinaison du rampant, l'allongement du thermosiphon ainsi que les sections d'ouvertures à l'entrée et à la sortie.

Les travaux réalisés sur les thermosiphons inclinés chauffés différentiellement ne sont très pas nombreux dans la littérature. En effet, les études sont généralement menées sur des thermosiphons verticaux ayant les parois actives soumises à des conditions de températures ou de flux, uniformes constantes et égales.

L'objectif principal de l'étude du thermosiphon sous les tuiles est de le représenter par des corrélations pour le débit d'air induit et les coefficients d'échanges convectifs dans un modèle de rampant de toiture global en période estivale. N'ayant pas trouvé dans la littérature une corrélation adéquate pour le débit d'air induit dans cette configuration particulière de thermosiphon incliné, le but de ce travail est d'étudier à travers une approche expérimentale basée sur des mesures par PIV (vélocimétrie laser), l'écoulement d'air par convection naturelle dans la lame d'air ventilée. Un travail de modélisation du thermosiphon est ensuite réalisé sous le code CFD et est validé par les résultats expérimentaux. Des corrélations pour le débit d'air induit et les coefficients d'échanges convectifs sont ensuite proposées pour être imposées comme sollicitations dans le modèle de toiture thermique global en période estivale et développé au chapitre 5.

Le dispositif expérimental permettant de mesurer les débits d'air induits par effet thermosiphon est constitué d'une cavité parallélépipédique en plexiglas transparent d'une longueur de 100 cm, d'une largeur de 60 cm et d'une épaisseur de 3 cm. La partie supérieure de la cavité est chauffée par deux panneaux de silicones. Les températures obtenues à l'intérieur de la cavité sur les surfaces supérieure et inférieure sont alors mesurées à différents niveaux par des thermocouples et utilisées plus tard comme entrées pour le modèle numérique réalisé sous le code CFD Fluent. Les essais sont effectués pour différents niveaux de

chauffage, trois longueurs de rampant (1, 2 et 3 m), deux inclinaisons (30° et 35°) et deux sections d'ouvertures (2 et 3 cm).

Un modèle numérique représentant le thermosiphon du dispositif expérimental est ensuite réalisé sous le code CFD. Sur les deux surfaces actives sont imposés les profils de température mesurés. Un rapprochement est noté entre les deux valeurs, expérimentale et numériques avec une erreur moyenne de l'ordre de 8 %. Ceci permet alors de valider le modèle numérique réalisé.

Les résultats sur le débit d'air montrent tout d'abord qu'une réduction du flux incident engendre des températures moyennes réduites pour les deux parois actives du thermosiphon et donc des débits d'air moins importants. Par ailleurs, une augmentation de l'écoulement d'air est observée avec l'augmentation de l'inclinaison par rapport à l'horizontale. En effet, une inclinaison plus prononcée donne un mouvement de convection naturelle plus important et des débits d'air plus élevés. D'autre part, une évolution quasi linéaire du débit induit est observée dans la plage de longueur allant de 1 à 3 m. En effet, le flux thermique incident, proportionnel à la surface de la cavité, augmente avec la longueur de la cavité ; étant le moteur de l'effet thermosiphon, le débit induit augmenterait. De plus, les pertes de charge linéaires qui augmentent avec la longueur de la cavité et qui résistent à l'augmentation du débit ne semblent pas avoir d'effets suffisamment importants pour infléchir la croissance du débit. Ainsi les seules pertes de charge qui influencent sensiblement l'effet de thermosiphon sont les sections d'ouvertures à l'entrée et à la sortie de la cavité. La température de l'air ambiant est également un facteur important. En effet les résultats montrent que le débit d'air augmente avec l'écart de températures entre la paroi froide et l'air ambiant. Les paramètres qui définissent l'écoulement d'air par convection naturelle dans ce genre de thermosiphon sont donc l'inclinaison, l'allongement de la cavité, les nombres de Rayleigh pour les deux parois, froide et chaude, la température de l'air ambiant et la section d'ouverture à l'entrée et à la sortie.

Après l'étude des paramètres intervenant dans la génération de l'écoulement à l'intérieur du thermosiphon et la validation du modèle numérique réalisé, plusieurs simulations numériques sont réalisées afin de calculer des points supplémentaires et obtenir une meilleure corrélation dans ces plages de paramètres. La corrélation établie par la méthode des moindres carrés englobe 90 % des résultats avec un écart de plus ou moins 20 %.

Pour le transfert thermique à l'intérieur d'un thermosiphon incliné chauffé par un seul côté, Azevedo a établi une corrélation pour les coefficients d'échanges convectifs à l'intérieur de la cavité en fonction du nombre de Rayleigh et de l'inclinaison. Etant donné que sa corrélation est valable pour un angle d'inclinaison supérieur à 45° et pour de plus grands allongements, les coefficients d'échanges convectifs obtenus par simulations numériques validées par les mesures PIV permettent de modifier la constante d'Azevedo pour adapter la corrélation dans les plages de données étudiées.

Enfin, les deux approches, expérimentale et numérique, nous ont permis d'obtenir des corrélations pour le débit d'air et les coefficients d'échanges convectifs à l'intérieur d'un thermosiphon incliné chauffé différentiellement. Ces corrélations représentant l'écoulement d'air et le transfert thermique dans la lame d'air ventilée seront introduits comme sollicitations dans le modèle thermique global représentant un complexe de toiture en période estivale intégrant un PMR et une lame d'air naturellement ventilée.

Modeling natural convection in a pitched thermosyphon system present in building roofs and experimental validation using particle image velocimetry

N. Chami et A. Zoughaib
Center for Energy and Processes (CEP), Ecole des Mines de Paris, Paris, France

Abstract

Attics in Europe are more and more used as a living room. In tropical regions, summer comfort in attics becomes critical when the roof system is badly designed. The European standards advise to form an open thermosyphon system into the roof under the tiles for many purposes. In order to evaluate the air channel's efficiency, an experimental study using a 2D-PIV system was carried out. A numerical model representing the natural convection within the thermosyphon was also developed. The predicted velocity distributions and the induced mass flow rate were in good agreement with the experimental results. Correlations for the air flow rate and heat transfer coefficients were proposed. The impact of the inclination, height, opening sections and Rayleigh number on the channel's efficiency was also investigated.

Keywords: PIV, pitched thermosyphon, CFD, heat transfer, natural convection, roof systems

Nomenclature

b	inter-plate spacing (m)
c	opening section (m)
cf	specific heat of air ($J.Kg^{-1}.K^{-1}$)
DT	temperature difference (K)
g	gravitational constant (9.81 $m.s^{-2}$)
h	convective heat transfer coefficient ($W.m^{-2}.K^{-1}$)
L	thermosyphon height (m)
Q	heat transfer rate (W)
S	cross sectional area (m^2)
T	temperature (K)
v	air velocity inside the channel (m/s)
x, y	cartesian coordinates
$\dot{m}$	mass flow rate ($kg.s^{-1}$)
Δt	time between two laser pulses (μs)

Greek symbols

λ	thermal conductivity ($W.m^{-1}.K^{-1}$)
β	coefficient of expansion (K^{-1})
μ	dynamic viscosity (Pa.s)
ν	kinematic viscosity ($m^2.s^{-1}$)
ρ	density ($kg.m^{-3}$)
θ	inclination angle, Fig.1 (°)

Dimensionless terms

A	aspect ratio (b/L)
Nu	average Nusselt number ($h.d/\mu$)
Pr	Prandtl number ($cf\,\mu\,/\lambda$)
Gr	Grashof number ($g\,\beta\,\Delta T\,d^3/\nu^2$)
Ra	Rayleigh number (Gr.Pr)

Indices

f	fluid
a	ambient air
∞	fluid environment
b	based on the inter-plate spacing
L	based on the thermosyphon height
w	plate surface
av	averaged
y	local
h	hot
c	cold
up	upper hot plate
low	lower cold plate

3.2 Introduction

Due to their numerous advantages, systems based on the heat transfer by natural convection are widely used in several engineering applications such as solar energy systems, electronic circuits cooling, air conditioning and natural ventilation in buildings. The passive systems called thermosyphons or solar chimneys attached to existing rooms in a building are the most common examples for ventilation applications. These structures are generally vertical or in some cases slightly tilted from the vertical position. They can produce natural movement of air in the building due the induced temperature differences by solar heating. Some of the chimney designs help to evacuate pollutants and humidity from the rooms; the buoyancy force drives the internal air upward throughout the chimney's exit; this movement assists fresh air to enter through the openings. For these purposes the solar chimney must be in contact with the internal air. Other chimneys are designed only to insert the collected solar radiation heat (in case of solar heating) or to evacuate the undesirable heat due to solar radiation (to reduce summer heat load), thus they are not related to the interior room air. Some of these particular passive solar heating designs are known as Trombe walls.

In this article, the studied system is not used to heat or ventilate the interior but to prevent from the warming of the roof system due to the solar heating. This thermosyphon is located under the tiles. The solar radiation increases the tiles temperature which heats up the air in the ventilated cavity setting up buoyancy force which induces the upward airflow circulation. The construction of this open air cavity in the roof system is specified by the European standards and the national building rules. It is designed to evacuate the humidity and therefore to protect the roof wood structure. It also helps to prevent the overheating of the tiles by solar irradiation; it evacuates the heated air from the roof system by the mean of passive ventilation.

The objective of this work is to study through an experimental set up the buoyancy-driven airflow generated in the thermosyphon implementing the PIV measurement technique. A CFD model representing this phenomenon is also developed and the results obtained for the air flow rate are validated by the experimental results. The experimental data together with additional numerical simulations allow us to propose correlations for the mass flow rate and heat transfer coefficients as a function of different parameters.

The developed correlations will be implemented in a 0D/1D thermal network type model in order to create a model for the whole roof system in static and transient conditions. Thus the main target is to represent the system with correlations for the mass flow rate and heat transfer coefficients.

3.3 State of the art

Roof systems are usually built with a ventilated air gap below the tiles and an airtight membrane or an underlay fixed on top of the insulation material (Figure 1). The implementation of a 3 cm minimum air gap is advised by the European standards and the national building rules [1]. The airtight membrane or underlay is advised to prevent the infiltration of snow, dust, rain and wind into the insulation and at the same time, if this underlay is in contact with insulation, it should be permeable to the water vapor in order to avoid condensation.

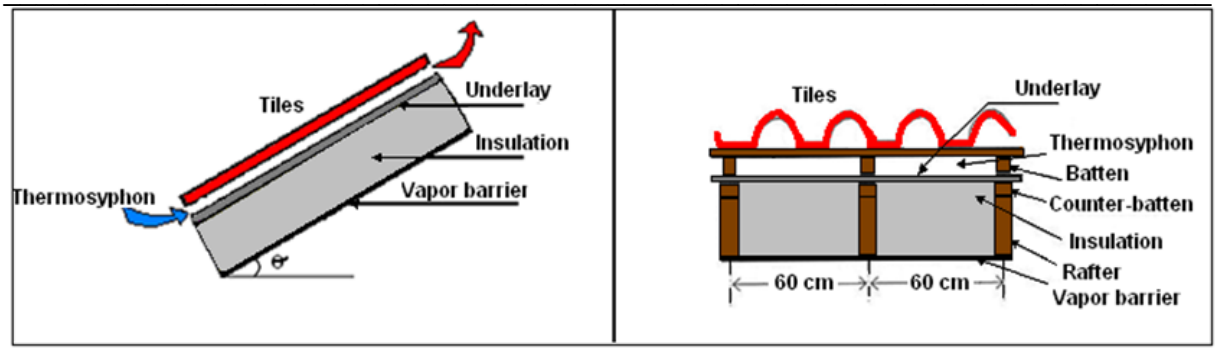

Figure 1 - Longitudinal and transversal section in the roof system.

Unlike forced convection, the buoyancy-driven natural ventilation usually has low flow rates and is difficult to control because it depends on various parameters like the incident solar radiation, the geometry and the inclination of the system. For this reason and in order to improve the understanding of the ventilation performance of the thermosyphon and its mass flow rate, the important parameters must be identified and their impact on the thermosyphon's efficiency must be studied.

In the literature, various experimental [2-7], analytical and numerical investigations [8-15] have been implemented to study the buoyancy-driven flow and heat transfer that occur inside thermosyphons of different configurations. In fact, various numerical studies, using 2D or 3D CFD techniques, were performed to characterize the air movement inside Trombe walls [16], thermosyphons [10, 17-18] and behind photovoltaic panels [19, 35]. Some authors conducted experiments to validate their models [20, 18, 21-24].

However, most of the studies investigate vertical thermosyphons which are simpler to construct and to study. The inclination could increase the exposure to solar irradiation and enhance the performance of the thermosyphon. Although extra tilt can also lead to a lower effective pressure head and smaller air flow rates. Few studies were found about the inclination [6, 10-11].

The objective of the studies of thermosyphon systems was mainly to optimize the aspect ratio of the thermosyphon for a maximum airflow induced [2-4, 6, 9, 25]. Few authors implement models or perform experiments to propose a correlation for the mass flow rate as a function of dimensionless parameters. The studies that developed 1D mathematical models based on the energy balance over the control volumes in the fluid and Bernoulli equations [12-15] were carried out for vertical thermosyphons and propose correlations for the air flow rate that can be used in a mathematical model.

Burek [5] experimentally investigated the natural convection flow inside a vertical solar chimney and inside a Trombe wall through a small experimental channel, one wall was uniformly heated and found that the air flow rate depends on: i) the heat input (proportional to the heat input with the power of 0.572) ii) the inter-plate spacing (proportional to the gap distance with the power of 0.712). However, like most of the studies, the impact of the height or the inclination on the thermosyphon's induced air flow rate was not investigated.

Besides the inclination and the dimensions, the thermal conditions of the thermosyphon's active walls are very important parameters for the mass flow prediction as well as for the heat transfer and for the temperature and velocity profiles. Concerning the investigation of the performance of thermosyphon systems, i) some studies in the literature considered the two plates symmetrically heated at the same uniform wall temperature (UWT) [2-4, 8-9, 18, 24,

26], ii) others at the same uniform heat flux (UHF) [9] and iii) some considered one wall uniformly heated and the other wall unheated or well insulated [5-6, 22-23]. Awbi [26] showed that the UWT assumption is valid for solar chimneys of gap-to-height ratio smaller or equal to 0.1 which corresponds to our case.

The experimental conditions stimulate what happens in the roof systems implementing a constant heat flux condition and a constant wall condition. This does not represent the real ambient conditions adequately. Although a constant heat flux is applied on the upper surface of the upper plate, the convective and radiative heat transfer between the surface and the ambient environment results a non uniform heat flux. Therefore the best simulation inputs considered in modeling are temperature profiles along the two plates. Due to the lack of correlations for the mass flow rate in tilted differentially heated thermosyphons, the approach followed in this article is based on PIV measurements that will determine the air flow rate induced. Having the upper plate uniformly heated while the lower one is not, temperatures inside the thermosyphon along the two plates are measured at different heights. The same temperature profiles are then used as a boundary limit in a CFD model along with the geometry and material properties and the results obtained for the air flow rate are validated by the experimental data. A correlation for the mass flow rate is then proposed and discussed. The model is used to propose a correlation for the heat transfer coefficient which is compared to the literature.

3.4 Experimental set up

The experimental apparatus used to measure the velocity field in a tilted thermosyphon is a 2D-PIV system. It is a non-intrusive flow measurement technique; it provides instantaneous velocity field measurement within the desired areas.

With this technique, the velocity field is determined by measuring the displacement of tracer particles inserted into the buoyancy-driven air flow. For that purpose, the particles of the seeding introduced in the test cell are illuminated, twice within a short time interval, by a pulsed laser light. The two locations of the tracer particles are recorded by a camera synchronized with the laser.

A double cavity Nd-Yag Solo III laser of 532 nm wavelength and 50 mJ pulse energy was used as a light source to illuminate a cross-section of the flow. A CDD camera, FlowSense 2M, with a resolution of 10 bits and 1600 x 1200 pixels located perpendicularly to the light sheet was used to capture the pair of particle images. The synchronization between the laser emission and the CDD was controlled by the Dynamic Studio software in order to obtain sequential pairs of particle images. Data analysis of the PIV was performed using the software package “Dynamic Studio”, described in detail in Dantec Dynamics user guide [27].

The experimental apparatus is shown in Figure 2. The laser plane is located at the centre of the cavity parallel to the flow and the camera is located at a distance of 0.68 m from the inlet cross-section of the cavity. The main components of the experimental set up are: i) the open cavity filled with air at atmospheric pressure, ii) the 2D-PIV system that includes the laser and the CDD camera, iii) the heating panels placed on the entire surface of the cavity’s upper plate and iv) the data acquisition system.

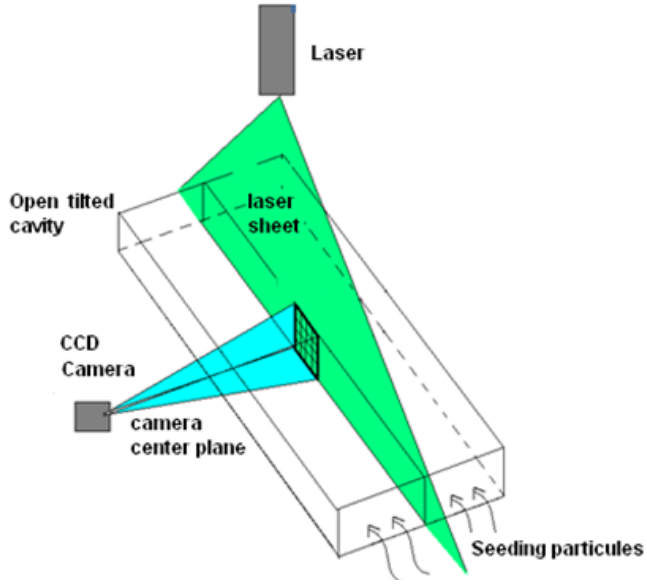

Figure 2 - Sketch and photo of the experimental set-up.

The cavity was made of transparent plexiglas to allow optical access for the CCD camera. The initial length of the channel is 1 meter; it is later on lengthened to 2 and 3 m. The channel has a constant width of 60 cm which is the most common distance between rafters. The inter-plate spacing is a constant value of 3 cm. The cross-section at the inlet and outlet takes two different values: 0.012 and 0.018 m^2.

The upper wall of the test cavity is entirely covered with two silicone heating panels. Each one can generate a power of 600 W under 230 V. The surface temperatures inside the cavity on the upper and lower plates were measured by J-type thermocouples at different levels of height from the bottom of the thermosyphon to its outlet. The ambient temperature was measured by one supplementary thermocouple.

The series of experiments were initiated with tracer particles suspended in the fluid. A smoke machine, Magnum 800, placed in front of the inlet section was used to insert the particles into the flow (figure 3). The particles were carefully chosen in order to follow the flow without deviation due to gravity.

Figure 3 - Photo of the smoke machine in front of the inlet section.

When the smoke is introduced in the thermosyphon (figure 4), a perturbation of the air motion inside the cavity occurs. The images are analyzed and the velocity profile is saved when steady conditions were observed again.

PIV analysis was conducted using cross correlation techniques, an interrogation area size of 32x32 pixels, with 50 % overlap.

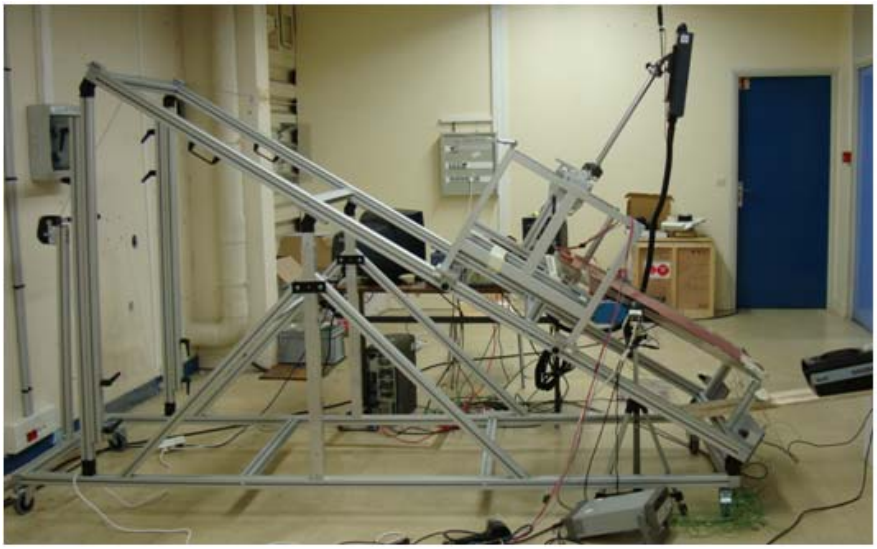

Figure 4 – Photo of the overall experimental test bench

3.5 CFD model

In differentially heated open cavities, the non-dimensional parameters that describe the natural convective flow in between the two parallel plates are: i) the number of Rayleigh Ra, ii) the Prandtl number Pr, iii) the aspect ratio A which is the inter-plate spacing b over the length L and iv) the inclination of the cavity (figure 5).

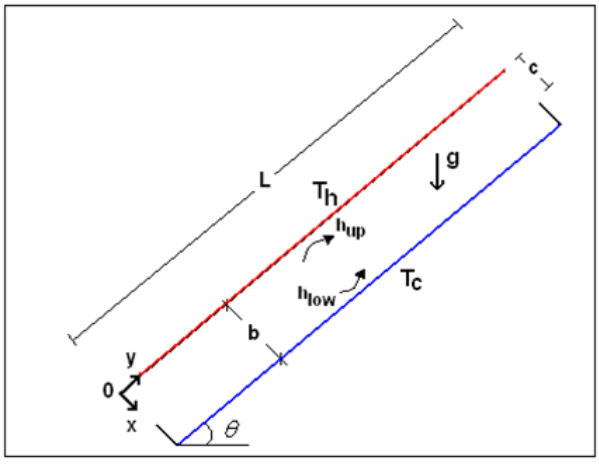

Figure 5 - CFD model representing the thermosyphon.

In our study, the working fluid is the air which has a constant Prandtl number equal to 0.71 thus the Nusselt number based on the inter-plate spacing of the thermosyphon is represented in the form of:

$$Nu_b = f(Ra_b, \frac{b}{L}, \theta) \qquad (3.1)$$

where the Rayleigh number based on the inter-plate spacing of the thermosyphon is defined as follows:

$$Ra_b = \frac{g\beta(T_W - T_\infty)b^3}{\nu^2}.\Pr \qquad (3.2)$$

β is the volumetric thermal expansion coefficient namely the change in the density of air as a function of temperature at constant pressure (K^{-1}), g is the gravitational acceleration (9.81 m^2/s), ν is the kinematic viscosity (m^2/s), T_W is the temperature of the plate, T_∞ is the ambient air temperature, and Pr is the Prandtl number. The thermophysical air properties in the Nusselt and Rayleigh numbers were all evaluated at the film temperature $(T_W + T_\infty)/2$.

According to the literature, the Rayleigh number based on the channel height is generally used to determine the flow regime in the thermosyphon. If the Rayleigh number becomes higher than a certain critical value, the buoyancy force becomes too important, compared to the viscous force acting on the fluid and the flow becomes turbulent.

$$Ra_L = \frac{g\beta(T_W - T_\infty)L^3}{\nu^2}.\Pr \qquad (3.3)$$

A numerical investigation of the natural buoyancy-driven fluid flow and heat transfer in the following thermosyphon has been carried out using the CFD code, Fluent. The equations of the steady, turbulent, incompressible and three-dimensional form of the conservation equations were solved for the air flow in the tilted thermosyphon using the Boussinesq approximation. This assumption imposes constant values in all thermophysical properties except for the density in the buoyancy force term of the momentum equation. It is also assumed that viscous dissipation is negligible. The $K-e$ turbulence model was chosen due to the high Rayleigh numbers.

For the inlet and outlet section of the thermosyphon, the pressure is set equal to ambient pressure and the inlet temperature is set equal to ambient temperature. For the two active walls, the temperature profiles obtained from the experiments were fixed as boundary conditions. The other walls were considered adiabatic.

An adequate mesh size was chosen for the three different cavity heights of the experiments (1, 2 and 3 meters). It was proven adequate by carrying out the grid independence test. Increasing the mesh size showed no changes in the velocity profiles for a certain section in the thermosyphon.

3.6 Results and discussion

3.6.1 Validation of the CFD model

The cases tested in the experimental set up using the PIV technique are shown in Table 1. Three lengths were tested, two opening sections, two inclinations and different wall-to-ambient temperature difference. The hot and cold temperatures, T_h and T_c, presented in Table 1 were computed, for each case, by averaging the readings of the different thermocouples placed inside the cavity along the length on both the upper and lower plate.

Table 1 – Cases tested in the experimental set up

case	Angle(°)	T_h (K)	T_c (K)	T_a (K)	DT (K)	L (m)	c (cm)
1	30	313.0	297.0	288	16.0	1	2
2	30	303.1	295.0	288	8.1	1	3
3	30	303.4	295.3	288	8.1	1	2
4	30	313.1	297.1	288	16.0	2	3
5	30	315.8	299.7	288	16.1	2	2
6	30	304.5	292.2	288	12.3	2	2
7	30	313.3	301.3	288	12.0	3	3
8	30	314.0	302.0	288	12.0	3	2
9	30	313.8	300.6	293	13.2	3	3
10	35	313.8	302.4	293	11.4	3	3
11	35	314.5	302.3	293	12.2	3	2
12	35	319.1	303.7	295	15.4	3	3
13	35	324.0	313.4	295	10.5	3	3
14	35	326.6	316.4	295	10.2	3	2

Figure 6 shows the results of the thermosyphon mass flow rate for different opening sections, lengths, inclinations and wall-to-ambient temperature differences. Both the values predicted by the CFD calculations and those obtained by the PIV measurements are represented.

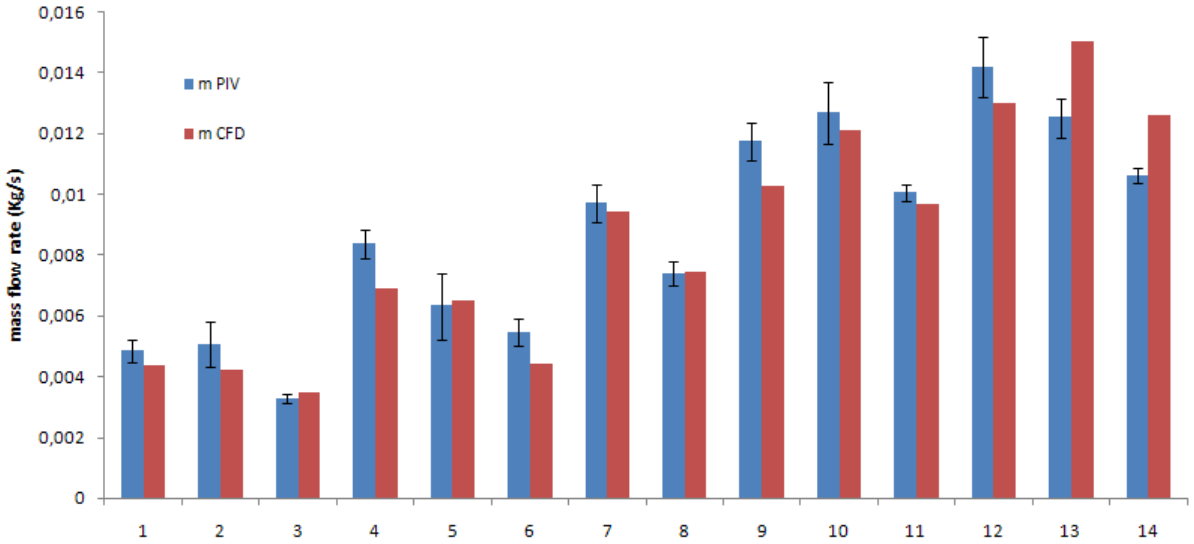

Figure 6 – Mass flow rate results of both experimental and numerical studies

For the PIV measurements, a maximum standard deviation of 0.11 % and an average standard deviation of 0.05 % were estimated. The comparison between the calculated and measured values shows a maximum difference of 19.7% and an average one of 10.3%.

The tendency of the mass flow rate progression as a function of the varied parameters is in good agreement with the literature. First of all, the reduction of the heat flux in both cases decreases the mean temperatures for the hot and cold plates and therefore decreased airflows. In addition, both results show that the mass flow rate induced in the thermosyphon increased with the inclination and the channel length. If the tilt angle is increased, the buoyancy-driven

flow is more intense generating an increased airflow. Moreover, the heat flux penetrating the thermosyphon is analog to the surface of the cavity, therefore the mass flow rate increases with the length. In addition, the linear pressure drop which increases with the length and opposes to the generation of bigger airflows doesn't seem to have impact on the thermosyphon for lengths up to 3 meters.

Another conclusion can be drawn from figure 6; as temperature difference between the cold wall and the ambient air (when this latter becomes close to adiabacity) increases, the mass flow rate increases.

The results also show than when changing the opening gap from 3 to 2 cm at the inlet and the exit of the air channel, the mass flow rate decreases by an average value of 18%. This is explained by the fact that when decreasing the opening sections, the pressure drop due to the inlet and exit sections increases, resulting lower mass flow rates.

In order to consider isothermal surfaces (for simplicity purposes) instead of the temperature profile, a set of numerical simulations was conducted using either the measured temperature profile or the averaged temperatures on cases of different heights (Figure 7). The results showed that the difference is negligible (around 3%) and that the assumption of isothermal plates can be applied for both the mass flow and the heat transfer.

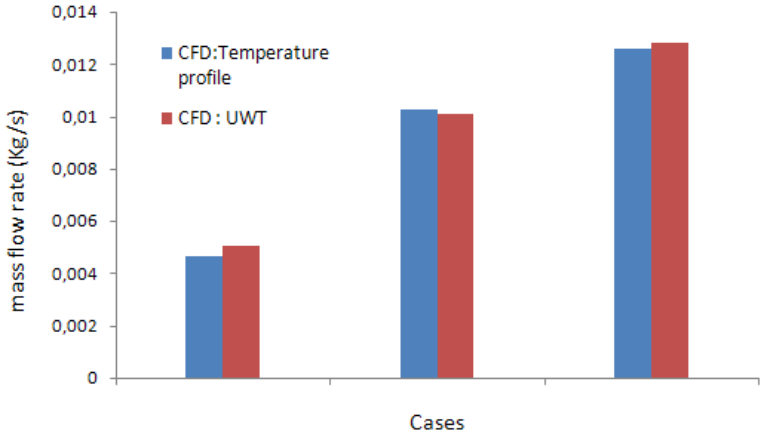

Figure 7 – Comparison between two CFD boundary conditions

The simulations performed in the following use the UWT instead of the temperature profile condition.

3.6.2 Correlation for the airflow rate

Both the experimental and numerical analysis showed that the mass flow induced in the channel is a function of the following parameters: the aspect ratio, the inclination, the upper and lower wall temperature and the ambient air temperature. To propose a correlation that is a function of the temperature difference between the plates and the ambient air, these three parameters were included into two dimensionless numbers. In fact, the heat transfer along the hot and cold plate in the air channel is defined with two Rayleigh numbers; one for the upper plate and the other for the lower one. Both are based on the cavity length and not on the spacing because the objective is to study the impact of the length on the performance of the thermosyphon, the inter-plate spacing is kept constant (3cm). The correlation for the mass flow rate is thus a function of i) the inclination, ii) the two Rayleigh numbers, iii) the aspect ratio of the thermosyphon and iv) the ambient air temperature.

After validating the model, additional numerical simulations were carried out in order to have more results for a wider range of parameters and to be able to propose an adequate correlation as a function of these parameters.

By using the least squares method on both the experimental and numerical results, the following correlation is proposed for the mass flow rate induced in the tilted air channel:

$$\dot{m} = 2{,}312E-5 \times \sin\theta \times (Ra_{L,h}{}^{0.4098} + Ra_{L,c}{}^{2.53E-9})^{0.6609} \times (\frac{c}{L})^{0.07} \times (\frac{T_\infty}{273.15})^{5} \quad (3.4)$$

where

$$Ra_{L,h} = \frac{g\beta(T_h - T_\infty)L^3}{\nu^2}.\Pr \quad (3.5)$$

And

$$Ra_{L,c} = \frac{g\beta(T_c - T_\infty)L^3}{\nu^2}.\Pr \quad (3.6)$$

Figure 8 compares the mass flow rates obtained by the correlation, numerically calculated and measured. The correlation established for the mass flow rate predicts 90% of the results within $\pm$ 20%.

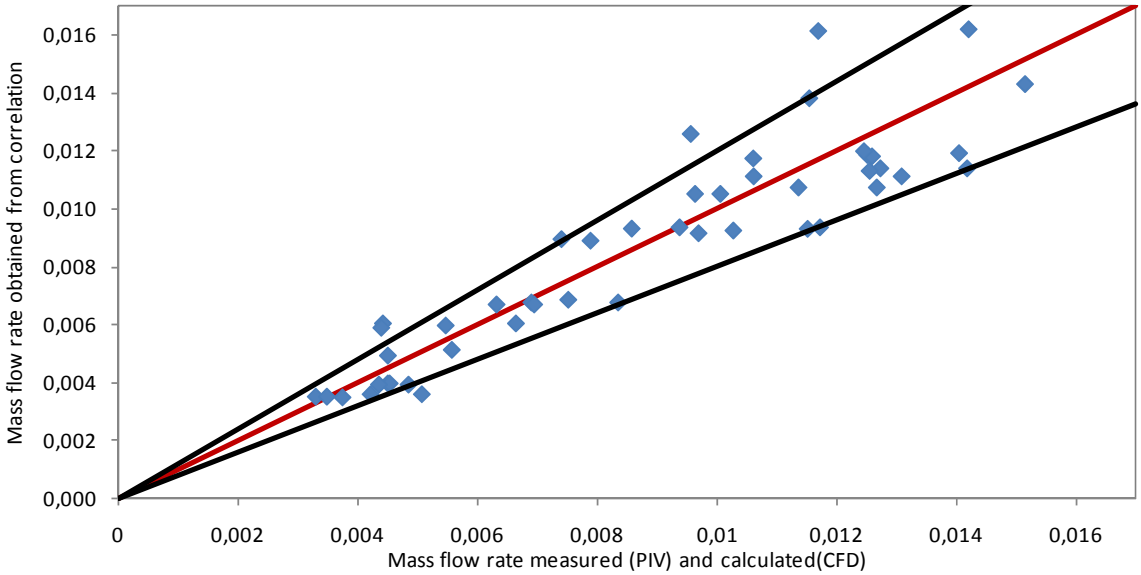

Figure 8 – Results for the mass flow rate.

The roof systems have usually a length between 4 and 6 m. In order to see if the correlation can be extrapolated to these lengths, two numerical simulations have been realized on two thermosyphons having the following lengths; 4 and 6 meters. The difference between the mass flow rate numerically obtained and the one calculated by the correlation was around 4% for both cases. Therefore, the correlation proposed is valid for an inclination angle that varies from 30 to 45° and an aspect ratio that varies from 0.005 to 0.03.

3.6.3 Correlation for the convective transfer coefficients

Most of the researches on the heat transfer coefficients inside thermosyphons are generally conducted for the vertical orientation like for instance [28-33]. Fewer authors investigate the heat transfer inside a thermosyphon for inclined positions. The only experimental investigation found in the literature on tilted channels is carried out by Azevedo [34] who studied the natural convection heat transfer inside a tilted thermosyphon filled with water (Pr=5) with variable aspect ratio, heating modes, angles and Rayleigh numbers.

In his experimental investigation, Azevedo [34] studied three heating modes; symmetrically heated, asymmetrically heated from above and from below. The roof system below the thermosyphon is usually insulated. This leads to the assumption that most of the incident heat flux is eliminated through the open air cavity by natural convection and therefore, the thermal flux passing into the attic is limited and can be considered small compared to the incident one. Our study can therefore be compared to the case of asymmetrically heating from above. For that specific heating mode, Azevedo defines a global heat transfer coefficient for the channel; it is given by the following relation:

$$h = \frac{Q}{S\Delta T} = \frac{Q}{S(T_W - T_{f,av})} \tag{3.7}$$

where Q is the convective heat flow (W) and S is the surface area (m^2) of the heated plate. $T_{f,av}$ is the average temperature of the fluid inside the channel and T_w is the average temperature of the heated plate.

The Nusselt number of the channel is defined as follows:

$$Nu_b = \frac{hb}{\lambda} \tag{3.8}$$

where λ is the thermal conductivity of the fluid ($W.m^{-1}.K^{-1}$).

The Rayleigh number used is expressed as follows:

$$Ra_b = \frac{g\beta(T_h - T_{f,av})b^3}{\nu^2}.\Pr \tag{3.9}$$

The correlation that Azevedo proposes is valid for all the investigated heating modes, inclinations ($45° < \theta < 90°$), inter-plate spacings (0.0437<b/L<0.109) and Rayleigh numbers (200< $((b/L)Ra_b)$ <2.105) with a divergence of $\pm$ 10%, it is given by the following equation:

$$Nu_b = 0{,}644\left[\frac{b}{L}Ra_b\cos(90-\theta)\right]^{0,25} \tag{3.10}$$

It shows that the heat transfer increases with the inclination and the Rayleigh number. On the other hand, the more the height of the cavity increases, the more the heat transfer in the cavity is decreasing.

The Azevedo correlation validity domain does not include the conditions explored in this study (0.01<b/L<0.03 and an inclination range that varies from 30° to 45°).

The experimental set up used in this study cannot be used to estimate the heat transfer coefficients along the upper and lower plate inside the thermosyphon. Thus, the experimentally validated CFD model is used to determine the heat transfer coefficients through the different simulated cases. The numerical results obtained from the CFD modeling were compared to the heat transfer coefficients calculated with Azevedo correlation (extrapolated out of its validity limits). The average heat transfer coefficient is obtained from the CFD numerical results by integration of the local convective heat exchanges:

$$h = \frac{\int h(x)S(x)dT(x)}{\int SdT} \tag{3.11}$$

The numerical results shown in Figure 9 confirm the conclusions drawn by Azevedo. The heat exchange coefficient increases with the Rayleigh number (based on the hot wall temperature) and inclination angle but decreases with the height of the thermosyphon.

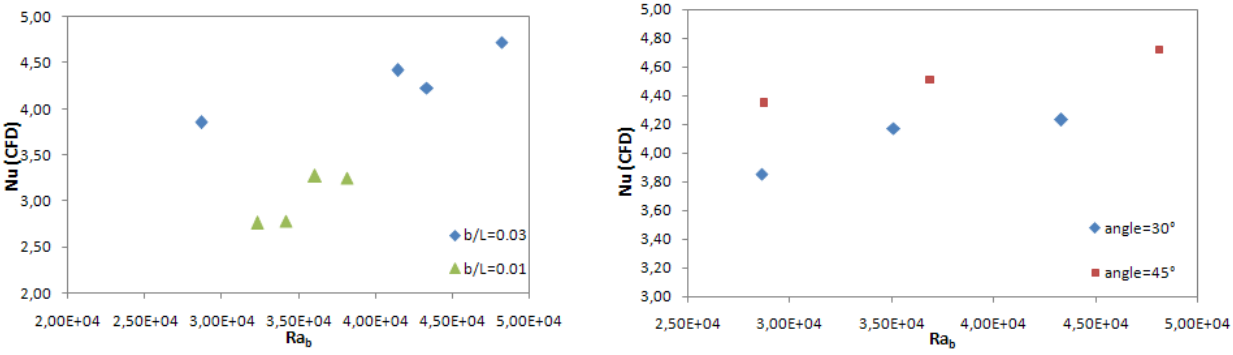

Figure 9 - Numerical Results of Nusselt numbers for different aspect ratios (left) and different inclination angles (right)

Figure 10 compares the heat transfer coefficients obtained from the CFD modeling and those calculated by Azevedo correlation for all the cases studied.

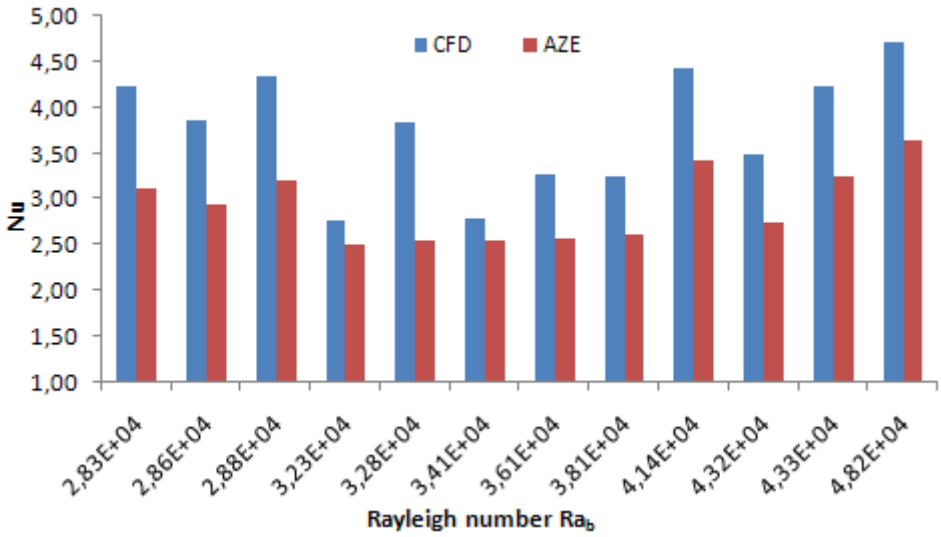

Figure 10 - Comparison of the Nusselt number results between Azevedo correlation and the numerical simulations.

The difference obtained between the two results is mainly because the correlation is valid for a minimum inclination angle of 45° and for an inter-plate spacing between 0.0437 and 0.109. Since our study investigate a smaller inter-plate spacing (0.01<b/L<0.03) and an inclination range that varies from 30° to 45°, additional series of numerical simulations were conducted in order to extend the range of applicability of the correlation for the heat transfer inside our channel.

The least squares method is used on the ten cases simulated in the CFD in order to propose a more suitable correlation for the air channel configurations for this study. The Nusselt numbers obtained from the numerical simulations were compared in Table 2 to the values calculated by Azevedo and to the ones obtained by the new correlation established using the least squares method.

Table 2 – Cases simulated in the CFD code.

case	angle(°)	L (m)	b/L	T_{amb} (K)	$T_{h.av}$ (K)	$T_{c.av}$ (K)	$T_{air.av}$ (K)	Nu (AZE)	Nu(CFD)	Nu (CORR)
1	30	1	0.03	288	311.7	296.7	293.5	3.40	4.23	4.02
2	45	1	0.03	288	313.3	298.2	292.9	3.72	4.72	4.40
3	30	1	0.03	288	304.1	296.0	292.8	3.06	3.85	3.63
4	40	1	0.03	290	311.7	296.7	294.2	3.58	4.42	4.23
5	30	2	0.015	288	320.5	310.5	300.2	2.86	3.49	3.38
6	30	2	0.015	288	315.6	310.6	300.6	2.67	3.84	3.16
7	45	3	0.01	288	320.4	310.4	302.2	2.73	3.25	3.23
8	45	3	0.01	288	320.4	315.4	303.1	2.69	3.27	3.18
9	45	3	0.01	300	330.4	320.4	311.6	2.65	2.78	3.14
10	45	3	0.01	300	330.4	325.4	312.5	2.62	2.76	3.10

Figure 11 represents the Nusselt number calculated by i) the CFD, ii) Azevedo's equation and iii) the new correlation proposed for all the cases studied.

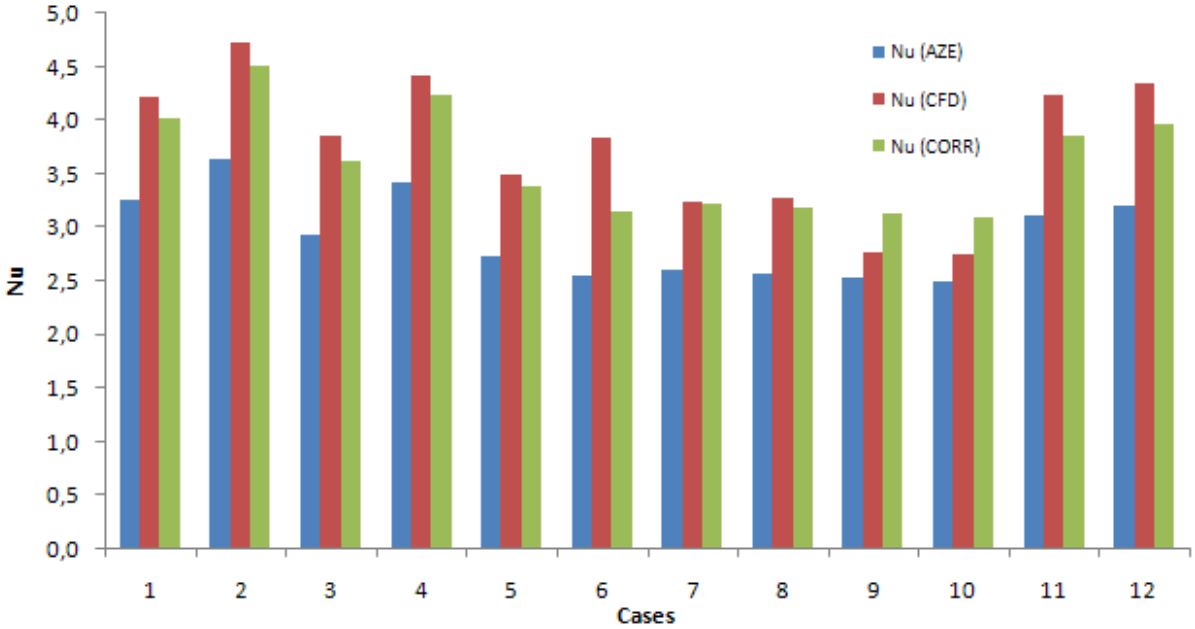

Figure 11 - Comparison of the Nusselt number results.

The correlation established for the range of aspect ratio studied in this article, which adapts the Azevedo correlation, gives an average standard deviation of 7% from the numerical results and is therefore more adequate:

$$Nu_b = 0{,}796\left[\frac{b}{L} Ra_b \cos(90-\theta)\right]^{0{,}25} \quad (3.12)$$

3.7 Conclusions

In this article, the performance of a tilted thermosyphon under the tiles was investigated through numerical and experimental investigation. The experimental set up was based on PIV measurements and was carried out in order to identify the important parameters that characterize the buoyancy-driven air flow inside the thermosyphon.

A numerical model for the air channel was developed using the CFD Fluent code. The mass flow rate results were validated by implementing 2D-PIV measurements. Both numerical and experimental results were used to propose a correlation for the mass flow rate induced that will be used as a solicitation in a thermal 0D/1D model.

A correlation from the literature for the heat transfer coefficients inside the thermosyhon was compared to the numerical results obtained from the CFD model. This correlation was adapted to the ranges of inclination angle and inter-plate spacing that defines the thermosyphon under the tiles.

Acknowledgments
The authors wish to thank the Isover Company for the financial support and cooperation.

References

[1] DTU 40.21 – Travaux de bâtiment – Couverture en tuiles de terre cuite à emboîtement ou à glissement à relief – NF P31-202-1/A2, August 2006
[2] W. Elenbaas, Heat dissipation of parallel plates by free convection, Physica, vol. IX, n° 1, pp 2-28, 1942
[3] A. Bouchair, Moving air using stored solar energy. Proceedings of 13TH National Passive Solar Conference, Cambridge, Massachusetts, 1988, 33-38
[4] A. Bouchair, Solar chimney for promoting cooling ventilation in southern Algeria. Building Service Engineering, Research and Technology 1994, 15(2), pp 81-93
[5] S.A.M Burek, A. Habeb, Air flow and thermal efficiency characteristics in solar chimneys and Trombe walls, Energy and Buildings, vol 39, pp 128-135, 2007
[6] Z.D. Chen, P. Bandopadhayay, J. Halldorsson, C. Byrjalsen, P. Heiselberg, Y. Lic, An experimental investigation of a solar chimney model with uniform wall heat flux, Build. Environ. 38 (2003) 893-906
[7] A. Dimoudi, A. Androutsopoulos, S. Lykoudis, Summer performance of a ventilated roof component, Energy and Building 38 (2006) 610-617
[8] HB. Awbi, G. Gan, Simulation of solar-induced ventilation. Renewable Energy Technology and The Environment 1992; 4: 2016-30
[9] B. Zamora, A.S. Kaiser, Optimum wall-to-wall spacing in solar chimney shaped channels in natural convection by numerical investigation, Applied Thermal Engineering, vol. 29, pp 762-769, 2009
[10] E.P Sakonidou, T.D Karapantsios, A.I Balouktis, D. Chassapis, Modeling of the optimum tilt of a solar chimney for maximum air flow, Solar Energy 82 (2008) pp 80-94

[11] D.J Harris, N. Helwig, Solar chimney and building ventilation, Applied Energy 84 (2007), pp 135-146
[12] K.S. Ong, A mathematical model of a solar chimney, Renew. Energ. 28 (2003) 1047-1060
[13] K.A.R Ismail, J.R Henriquez, Simplified model for a ventilated glass window under forced air flow conditions, Applied Thermal Engineering, vol 26, pp 295-302, 2006
[14] Aude Lacena-Neildez, Thèse Modélisation et etude expérimentale des échanges de chaleur dans des composants innovants de batiment industriels, 2000
[15] R. Bassiouny, N.S.A. Koura, An analytical and numerical study of solar chimney use for room natural ventilation, Energy and Buildings 40 (2008) 865-873
[16] G. Gan, S.B. Riffat, A numerical study of solar chimney for natural ventilation of buildings with heat recovery, Appl. Therm. Eng. 18 (1998) 1171-1187
[17] A.M Rodrigues, A. Canha de Piedade, A. Lahellec, J.Y Grandpeix, Modelling natural convection in a heated channel for room ventilation, Building and Environment, 35, pp 455-469, 2000
[18] E. Bacharoudis, M.G. Vrachopoulos, M.K. Koukou, D. Margaris, A.E. Filios, S.A. Mavrommatis, Study of the natural convection phenomena inside a wall solar chimney with one wall adiabatic and one wall under a heat flux, Applied Thermal Engineering 27 (2007) 2266-2275
[19] B. Moshberg, M.Sandberg, Flow and heat transfer in the air gap behind photovoltaic panels, International Journal of Renewable and Sustainable Energy Reviews, 2, pp 287-301, 1998
[20] G. Gan, A parametric study of trombe walls for passive cooling of buildings, Energy Buildings, 1998; 27, pp 37-43
[21] C. Afonso, A. Oliveira, Solar chimneys: simulation and experiment, Energy and Buildings 32 (2000) 71-79
[22] M. Sandberg, Cooling of building integrated photovoltaics by ventilation air. In: Proceedings of HybVent Forum 99, The University of Sydney, Australia, 28 september 1999. P 10-8
[23] H. Fath, Development of a natural draft solar fan for ventilation of greenhouses in hot climates. In t Journal of Solar Energy 1993; 13:237-48
[24] P.I Betts, I.H Bokhari, Experiments on natural convection of air in a tall cavity, In: IAHR workshop on flow modeling, Paris, vol V, 1996, pp 25-26
[25] B. Morrone, A. Campo, O. Manza, Optimum plate separation in vertical parallel plate channels for natural convective flows : incorporation of large spaces at the channel extremes, International Journal of Heat and Mass Transfer, vol 40, No 5, pp 993-1000, 1997
[26] H.B. Awbi, Design consideration for natural ventilated buildings. Renewable Energy 1994;5:1081-90
[27] Dynamic Studio software and Introduction to PIV instrumentation, DantecDynamics GmbH, Publication number: 9040U3625
[28] A. Mitra, T.K. Dutta, D.N. Ghosh, Natural convective heat transfer in water enclosed between pairs of differentially heated plates, Heat Mass Transfer (2008) 45: 187-192
[29] ERG Eckert, WO Carlson, Natural convction in an air layer enclosed between two vertical plates with different temperatures, Int J Heat Mass Transfer 2:106-120, 1961
[30] M. Jakob, Heat transfer, vol. 1, Wiley, New York, pp 536-539, 1949
[31] RK MacGregor, AF Emery, Free convection through vertical plane layers-moderate and high Prandtl number fluids. J Heat Transfer 91: 391-403
[32] E.M Sparrow, GM Chrysler, LF Azevedo, Observed flow reversals and measured-predicted Nusselt numbers for natural convection in a one-sided heated vertical channel; J Heat Transfer 106: 325-332
[33] LFA Azevedo, EM Sparrow, Vertical-channel natural convection spanning between the fully-developed limit and the single-plate boundary-layer limit, Int J Heat Mass Transfer 28: 1847-1857
[34] L.F.A Azevedo, E.M. Sparrow, Natural convection in open-ended inclined channels, Journal of heat transfer, vol. 107, pp 893-901, November 1985
[35] A. Guiavarch, B. Peuportier, Photovoltaic collectors efficiency according to their integration in buildings, Solar Energy, vol 80 n°1 pp 65-77, 2006